CHAPTER 3

DESIGN OF A WIDE-FIELD FINITE-CONJUGATE MICROSCOPIC IMAGING PLATFORM ON SMARTPHONE

This chapter discusses the design of a high resolution, wide-field multi-modal finite-conjugate microscopic imaging system on a phone. By using the embedded imaging sensor and other functional components, the phone has been converted into a 3f finite-conjugate imaging tool. The designed system utilizes the built-in camera for recording of the microscopic images. The LED flash of the phone has been used as an optical source. With facile design approach by integrating 3D-printed parts and off-the-shelf optical components, three dynamically adaptable modes of imaging, namely transmission BF, OIDF and TIRDF, have been demonstrated on a single platform. The design parameters such as magnification and optical resolution as well as the construction of the device have been discussed thoroughly. The applicability of the platform has been demonstrated through imaging of different biological sample. Also, the results have been compared with the standard laboratory microscope.

3.1 Background

The illumination technique is one of the most critical determinants of the imaging performance of any microscopic system. Based on the requirements of the specimen, the illumination technique needs to be dynamically adaptable. For instance, unstained specimens such as mammalian cells are more clearly visible under DF or phase-contrast (PC) illumination than under BF illumination. Traditionally, in all modern laboratory optical microscopes, the Köhler illumination method is being used,

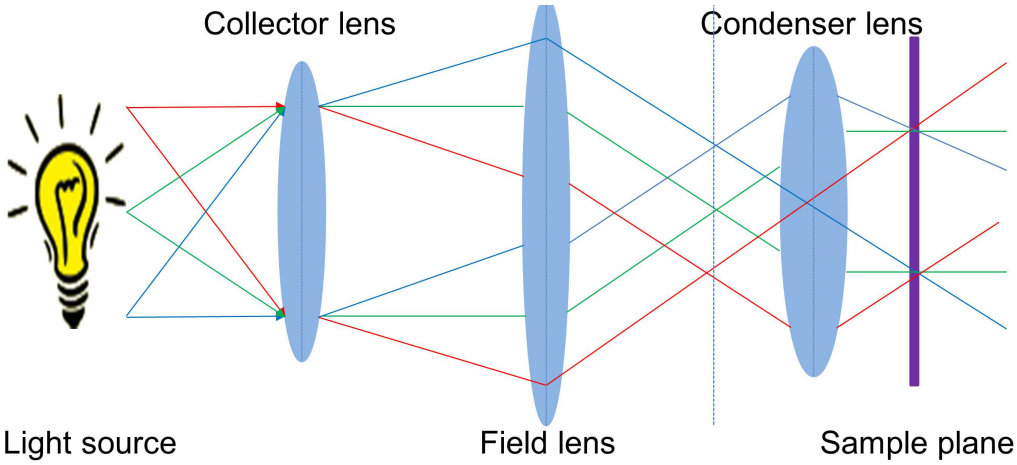

Figure 3.1: Basic optical configuration of the Köhler illumination setup.

which was introduced by August Köhler in 1893 [1]. The basic optical design of this illumination technique is illustrated in figure 3.1. The technique produces extremely even illumination by collecting the light from the source throughout the entire FoV. For different imaging conditions, however, it requires additional components such as filters and physical masks before the condenser lens of the Köhler illumination setup to produce spatially-modulated illuminations. For instance, in DF imaging mode, a specialized opaque disc (spider stop) is introduced on the aperture focal plane of the condenser lens to create a hollow cone of light so that only the scattered light from the specimen can enter the objective lens [2–4]. Though these techniques allow direct visualization of colorless and unstained biological samples, the use of additional elements makes the system very expensive and complex, thus restricting its feasibility for use in resource-poor settings.

Over the past few years, numerous works have been reported that developed smartphone-based portable microscopes for personalized medicine, healthcare, environmental monitoring, and education [5]. An inexpensive and lightweight microscopic imaging device can immensely improve and untangle the way of various microscopic examinations. In the beginning, the low-cost microscopes were realized for the mass by simply adding an objective lens atop to the camera module of a phone. Since then, many lens-free [6, 7] and lens-based [8–12] microscopic imaging on smartphone platforms have been demonstrated for blood cell imaging, diagnosis of malaria, sickle cell anemia, and detection of water-borne parasites like Giardia lamblia, soil-transmitted helminths in stool samples. In the lens-free approach, the miniature objective lens is removed from the camera module of the phone and the imaging principle is based on the digital inline holography technique. While this approach provides a compact and robust microscope design suitable for infield applications, the image reconstruction is computationally expensive for mobile devices. On the other hand, in the lens-based approach, the performance of the imaging systems is determined by the optical de-

sign of the systems, where increased spatial resolution results in the limited FoV. In spite of that, their effectiveness has been substantiated for many onsite applications where resources are the major constrain. However, most of the reported imaging systems were designed to be optimally used in a single mode such as BF, DF or fluorescence based imaging. Besides, many of these tools use external LEDs and batteries which eventually cause an increment on the cost, size and complexity of the device, thus limiting its feasibility for which it was designed. Nevertheless, few exceptions are there that demonstrate multi-mode microscopic imaging on smartphone platform but with complex implementation processes. A truly and convenient low-cost, compact and robust microscopic device demands the simple realization and execution of the system. In this chapter, the development of a simple 3D-printed low-cost, compact multi-modal microscopic system is discussed that utilizes the embedded CMOS imaging sensor and LED flash of a smartphone for detection and illumination respectively. Following schemes have been accomplished in this proposed imaging system:

1. At first a simple $3f$ optical imaging configuration, also termed as finite-conjugate system will be constructed by integrating a miniature and inexpensive objective lens to the phone camera module.

2. The LED flash lamp of the phone has been used as an optical source for the imaging system for realization of three different microscopic modes-BF, OIDF, and TIRDF. The proposed approach has an ability to convert rapidly from one imaging mode to another by simply reconfiguring the illumination setup in the system. For DF imaging, it requires a relatively intense beam of light since only the scattered light signals from the samples are recorded by the objective lens. In the present system, a pair of flexible plastic optical fibers has been used to guide the light from the LED flash of the phone to the specimen for imaging to be captured in BF, OIDF and TIRDF modes.

This dynamically adaptable transmission feature of the proposed system offers an important advantage of imaging those samples that are optically translucent in nature and cannot be viewed under BF mode. The usability of the designed microscope will be discussed through imaging of micro-beads, nanoparticles, biological cells and other living microorganisms.

3.2 Working principle

3.2.1 Description of the imaging and magnification system

The smartphone platform microscopic system has been constructed as a compact and portable standalone device where both the imaging sensor and LED flash has been

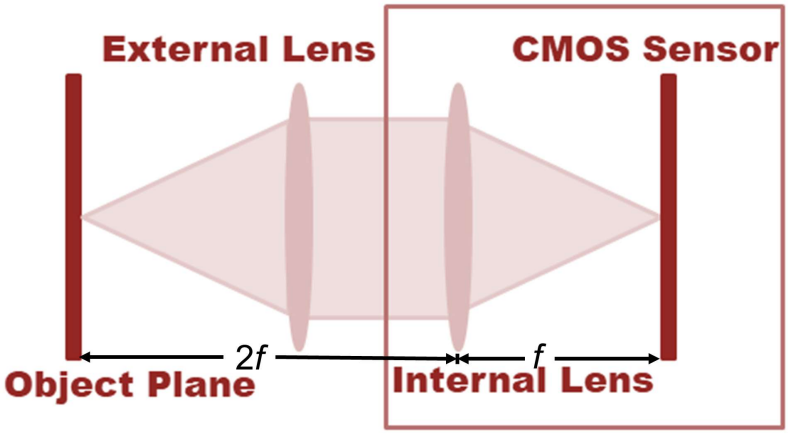

Figure 3.2: Realization of a finite-conjugate optical configuration on smartphone.

utilized. For the development of the proposed imaging system, Redmi K20 smartphone from Xiaomi Inc. has been used. This phone is equipped with 48 megapixel (MP) Sony IMX582 CMOS imaging sensor with superpixel technology where four pixels of 0.8 μm are combined to form a single large pixel of 1.6 μm. The camera sensor has a dimension of 8 mm (diagonal). It is embedded with 1/1.75 aperture lens and has an optical zoom of 2×. To convert the smartphone into a microscope with high FOV and spatial resolution, we use the rear camera lens (FL = 4.12 mm, NA = 0.23, f/2.2) of iPhone 5s as an objective lens in the designed setup. This lens has a magnifying power of ($\frac{250mm}{FL}$) 60× and is readily available in online market at a relatively low price (∼USD 5). The reason for using this specfic lens in the present system is that it is well-corrected lens for all kinds of aberrations and distortions that may present in an optical lens. To achieve the desired magnified image of an object in the imaging plane, this lens has been mounted in reverse orientation in the optical setup and is kept aligned with the optical axis of the camera-lens of the phone. This will create a finite-conjugate or $3f$ optical imaging system as shown in figure 3.2. The implementation of this configuration is easy and it provides rational spatial resolution with a relatively high FoV. Figure 3.3 represents the schematic optical configurations of the proposed microscopic system which have been used for BF, OIDF and TIRDF imaging for the present work.

3.2.2 Description of the illumination technique

The use of the LED flash to design a trans-illuminated microscopic system is a bit tricky as it is facing in the same direction of the camera. Besides, the LED flash is separated from the camera, only by few millimeters. In the present optical setup, two pieces of plastic optical fibers of diameter 1 mm (Edmund Optics part no: #57096, NA ∼ 0.51) each of length 15 cm has been used to guide the light from the phone LED

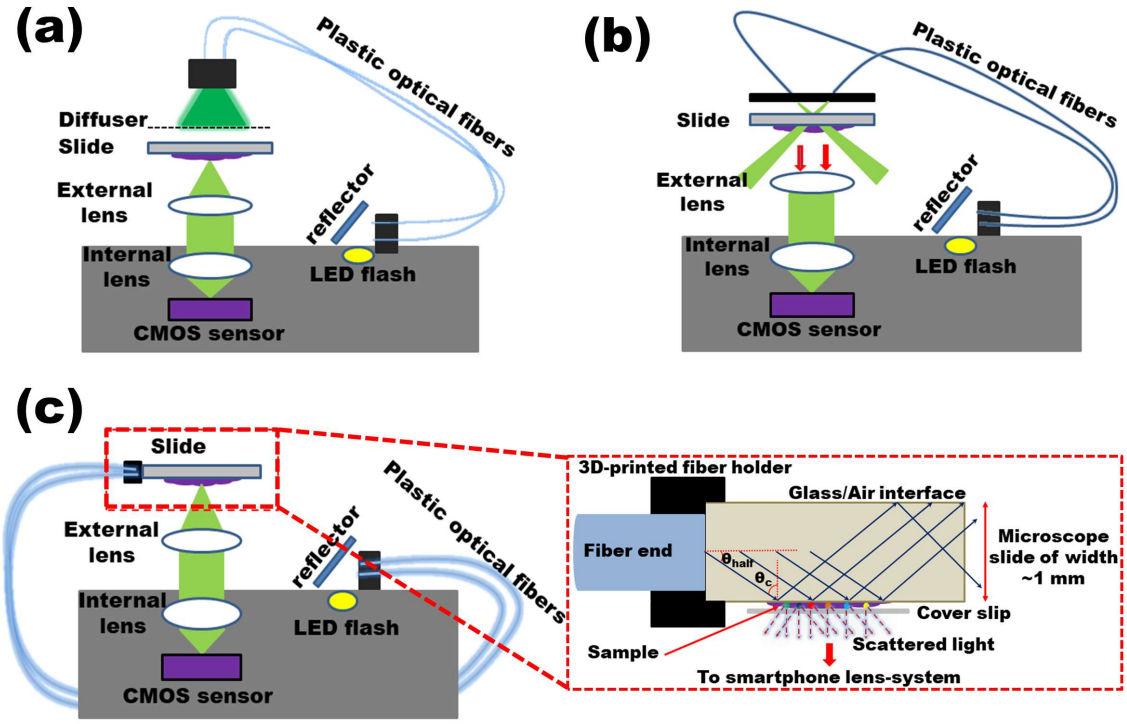

Figure 3.3: Schematics of the proposed smartphone microscopic imaging system. (a) BF illumination, (b) OIDF illumination and (c) TIRDF illumination respectively. The inset in figure (c) shows the guided light from the optical fibers propagates in the lateral direction of the glass slide through the process of total internal reflection.

flash to the specimen. A reflector of dimension 4 mm × 4 mm has been fabricated by coating silver film on a metal plate and has been placed at an angle of 45° in front of the LED flash. The reflected light at 90° to the direction of the incoming light is directly coupled to the fibers and the output light signal from these fibers has been used to illuminate the specimen. Owing to the flexible nature of optical fibers, the designed system offers the advantage of rapidly converting from BF to OIDF and TIRDF imaging mode simply by changing the position of the light guiding fibers in the setup.

For BF imaging, the end faces of the fibers are kept at a distance of 20 mm from the specimen as shown in figure 3.3(a). For uniform illumination, a diffuser made of 1 mm thick nylon sheet has been placed at a distance of ∼15 mm from the fiber ends and trans-illuminate the sample. For DF imaging, two methods have been employed. (i) In the first method, an oblique illumination has been performed to obtain the OIDF images and this is shown in figure 3.3(b). The optical fibers have been placed at an experimentally optimized illumination angle of 56° on either side of the optic axis of the designed setup. The direct light from the fibers will go straight through the specimen slide without entering the objective lens and only the forward-scattered or refracted light from the specimen will enter the objective lens. This will make the

objects bright against the dark background. For this imaging mode, the fibers are kept at a distance of 5 mm from the specimen. (ii) For TIRDF imaging, the DF illumination has been accomplished by employing total internal reflection technique through guiding the light along the lateral direction of a microscopic slide. As shown in the figure 3.3(c), both the light guided optical fibers are coupled to one side of the microscopic slide (dimension: 75 mm × 25 mm × 1 mm). For the propagated light through the slide whose incidence angle are greater than 41.2° (critical angle, $\theta_c = \sin^{-1}\frac{n_{Air}}{n_{Glass}} = 41.2°$ where, $n_{Air} = 1$ and $n_{Glass} = 1.518$) will undergo total internal reflection (TIR). On occurrence of TIR, an evanescent field will be generated at the interface and creates a localized illumination field. The microscopic particles present on the slide scatter strong forward signal which can be captured by the designed optical setup [13]. Since the evanescent field extends only to several hundred nanometers, forward scattered signal from the objects will appear bright against a dark background.

3.3 Device construction

Optomechanical design and fabrication

The goal of the work was to engineer a compact phone based microscopic platform with simple design approach that can be rapidly assembled with the least possible number of parts. The system should be mechanically stable that include a specimen holder with sufficient focusing accuracy. The optomechanical parts of the microscope have been constructed using 3D printing technology to hold all the essential components. It allows fabricating the microscopic system at affordable rate which is essential for the deployment in low-resource settings.

Figure 3.4(a), (b), and (c) shows the 3D rendering of the microscopic system in three different imaging modes. The design of the proposed system is performed on ZW3D – a CAD software. The designed files are then exported in .stl (Stereolithography) format. The layer resolution of the files was controlled using 'Ideamaker' slicing engine software and exported in 3D-printable format. The printing has been performed in FDM 3D printer (Raise3D, model N2). This specific 3D printer has a nozzle diameter of 400 μm with a maximum layer resolution of 10 μm having position accuracy of 1.25 μm in Z-direction and 1.25 μm X/Y step size. In the present work, PLA (Polylactic Acid) polymer filament was used for printing of the parts of the optical setup. Black filament has been used to avoid any color interference and also to optically shield the setup from ambient light. The 3D-printed setup holds the objective lens, specimen slide and other optical components and can be attached to the rear camera of the phone as a plug and play device. The prototype of the

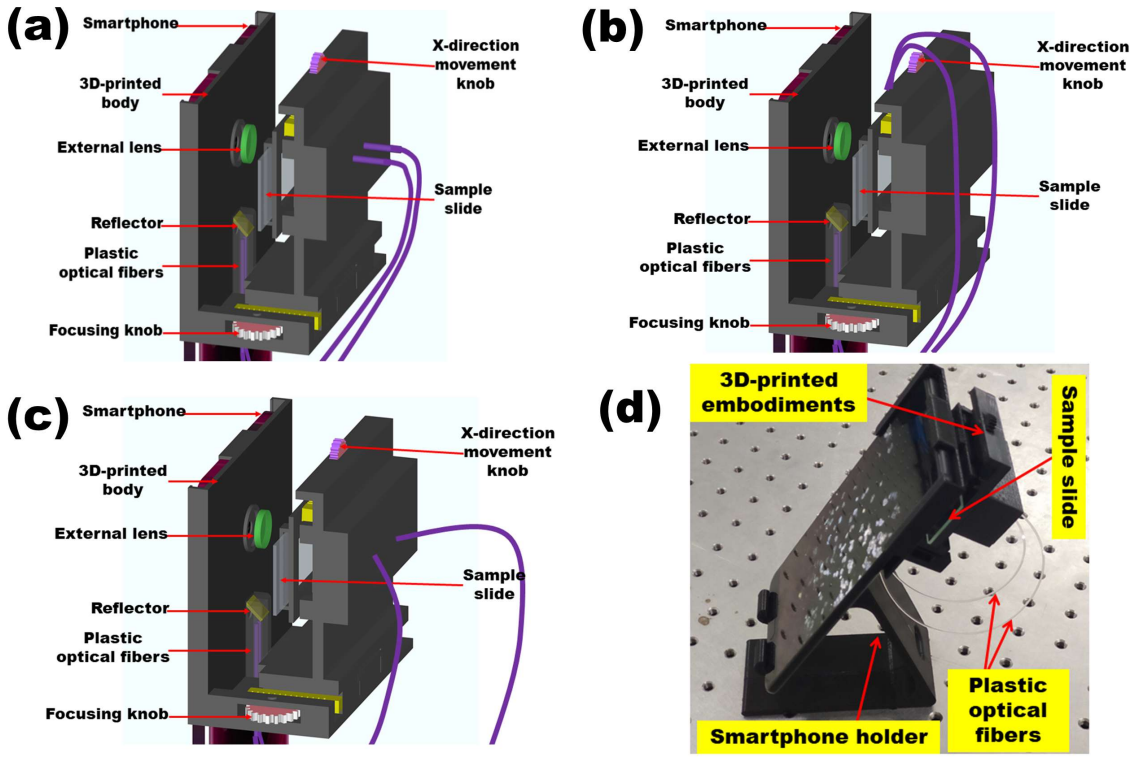

Figure 3.4: Smartphone microscopic device. 3D layout of the smartphone platform imaging system (a) in BF mode, (b) in TIRDF mode, (c) in OIDF mode, and (d) represents the photo image of the designed setup developed for the present work.

designed platform is shown in figure 3.4(d).

3.4 Optical characterization

Magnification, resolution and field-of-view

The net optical magnification of the finite-conjugate configuration, which is defined as the ratio of the focal lengths of the phone's internal camera lens (FL = 4.77 mm) to the external lens (FL = 4.12 mm) is calculated to be 1.16×. This magnification is found to be varying axially away from the optical axis. The considered phone has a screen size of 6.39 inch (diagonal) with an aspect ratio of 19.5:9. The unzoomed image has a digital magnification ($M_{digital} = \frac{ScreenSize}{SensorSize}$) of 20.3× when displayed on the phone screen.

To estimate the lateral resolution of the designed microscopic system, a standard 1951 United State Air Force (USAF) resolution test target has been imaged with the designed tool. Following equation has been used to measure the resolution of the device.

$$Resolution(\frac{lp}{mm}) = 2^{GN+\frac{EN-1}{6}} \tag{3.1}$$

where, GN (group number) and EN (element number) refers to the clearly resolvable

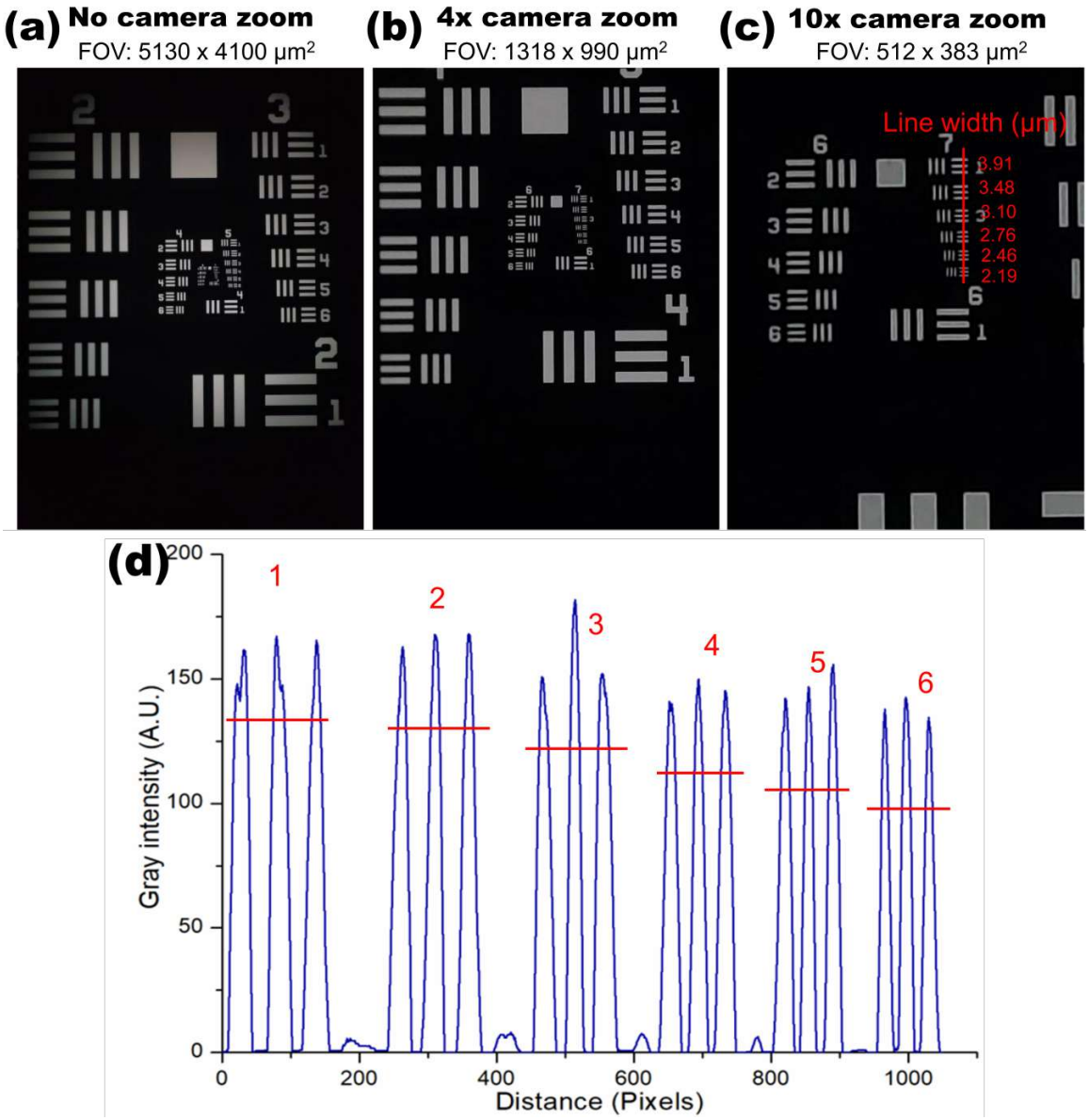

Figure 3.5: Characterization of the designed tool for evaluation of spatial resolution and FoV. Image of 1951 USAF resolution test target captured by the designed tool under BF illumination (a) without using digital zoom, (b) with 4× digital zoom and (c) after considering 10× digital zoom of the camera app. (d) represents the intensity profiles of the lowest resolving group (group 7 elements 1 - 6).

white and black bars of the test target. The iPhone 5s camera lens has $f/2.2$ aperture lens which is equivalent to NA = 0.23. Theoretically, the maximum achievable diffraction-limited resolution at the optical axis using this lens is 1.45 μm for $\lambda = 550$ nm ($R_{diff} = \frac{0.61\lambda}{NA}$). Experimentally, it was observed that the microscopic system can spatially resolve the highest line element i.e. group 7 element 6 of the test target easily which is equivalent to 228.1 line pairs per millimeter (lp/mm). The images of the test target are shown in the figure 3.5 where figure 3.5(a), (b) and (c) are taken with no camera zoom, 4× camera zoom and 10× camera zoom respectively. Figure 3.5(d) shows the intensity plot of the line elements of group 7 of the test target. Clearly, the designed microscopic system provides a lateral resolution well below 2 μm. Due to the presence of Bayer color filter array in the imaging sensor and digital sampling of the images, the actual resolution of the designed microscopic system may be different. With the present smartphone, the camera sensor in normal 'Photo' mode has a pixel pitch of 1.6 μm, which suggests a Nyquist-limited sampling resolution [11] of 3.9 μm. But in '48 MP' mode, it has a pixel pitch of 0.8 μm that gives a sampling resolution of 1.95 μm. The FoV of the microscopic system is calculated to be 5130 μm × 4100 μm, when no camera zoom was used.

3.5 Practical imaging using the smartphone microscopic device

To evaluate the performance of the proposed microscopic device, different specimens such as micro-particles, biological samples and microorganisms have been imaged under different illumination conditions and estimated the contrast and signal-to-noise ratio (SNR) values. For any imaging system the contrast can be estimated using the following equation:

$$C = \frac{I_{max} - I_{min}}{I_{max} + I_{min}} \tag{3.2}$$

where, I_{max} is the maximum intensity of the specimen and I_{min} is the minimum intensity values of the background. Again, SNR is estimated using following equation [14]:

$$SNR = \frac{I_{specimen} - I_{bg}}{\sigma_{bg}} \tag{3.3}$$

where, $I_{specimen}$ is the average intensity of the specimen, I_{bg} is the average intensity of the background and σ_{bg} is the standard deviation of the background.

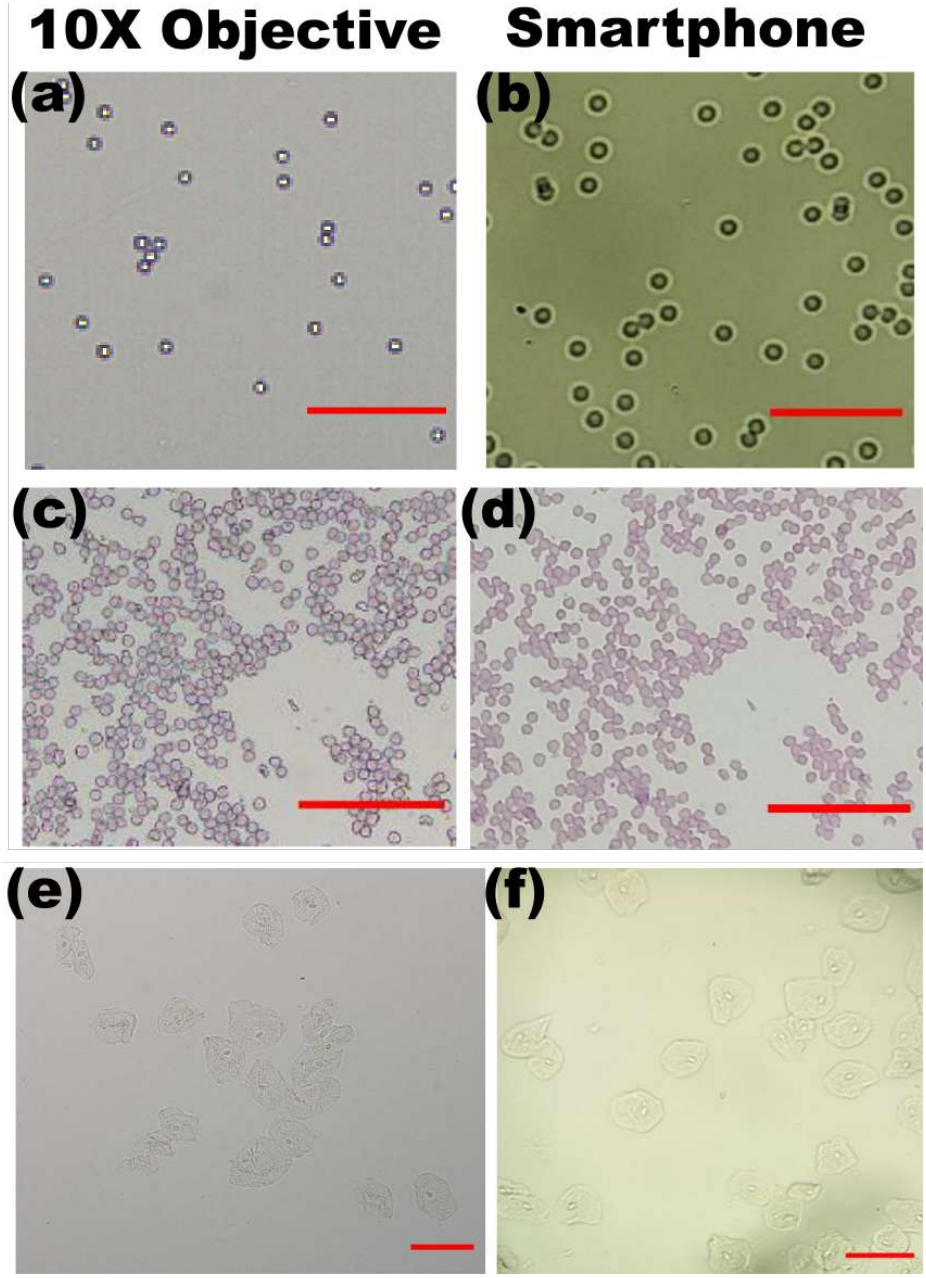

Figure 3.6: Comparison of imaging characteristics by standard optical microscope (10×/0.25NA objective lens) and the designed BF smartphone microscopic setup. (a), (b) 5 μm silica beads. Scale bars are 40 μm. (c), (d) images of Leishman stained blood smear. Scale bars are 100 μm. And (e), (f) unstained HECC cells. Scale bars are 100 μm.

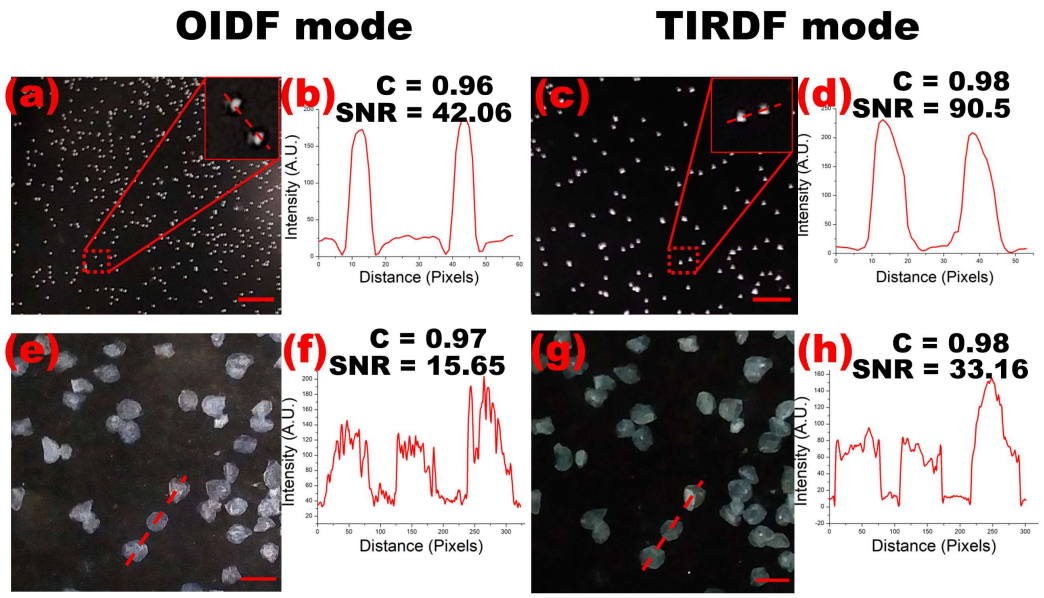

Figure 3.7: Applications of smartphone microscopic device for imaging of biological samples under different DF illumination mode. Zoomed-in and cropped images of microbeads captured (a) under OIDF illumination, (c) under TIRDF illumination mode. Scale bars are 50 μm. (b) and (d) represents the intensity profiles of the inset figure in (a) and (c) respectively. Zoomed-in and cropped images of HECC cells under (e) OIDF illumination mode and, (g) TIRDF illumination mode while (f) and (h) show the intensity distribution of the marked region respectively. Scale bars are 100 μm.

3.5.1 Application to imaging of micro-particles and biological cells and comparison with laboratory microscope

Figure 3.6(a)-(f) represent the BF images of 5 μm silica microbeads, a Leishman stained thin blood smear and unstained human epithelial cheek cell (HECC)s. These have been imaged with a 10×/0.25NA objective lens on a laboratory grade microscope (Carl Zeiss's Primo Star) (figure 3.6(a), (c), (e)) and with the present smartphone microscopic system (Figure 3.6(b), (d), (f)) respectively. The contrast and the SNR values for microbeads are estimated to be 0.36 and 7.8 for laboratory microscope while these values are found to be 0.61 and 25.8 when recorded with the smartphone respectively. For the red blood cells (RBCs), the contrast and SNR values are measured to be 0.16 and 15.07 for the standard microscope while these values are found to be 0.28 and 15.24 with our designed tool. The enhanced performance of the designed BF microscope over its commercial counterpart is attributed to the improved imaging sensor of the phone and the built-in optics in it. HECCs are translucent mammalian cells and produce very less contrast under BF illumination condition. Figure 3.6(e) and (f) represents the BF images of HECCs captured by the laboratory microscope and the designed smartphone microscope respectively. The contrast values of the HECCs are calculated to be 0.036 and 0.075 for the optical microscope

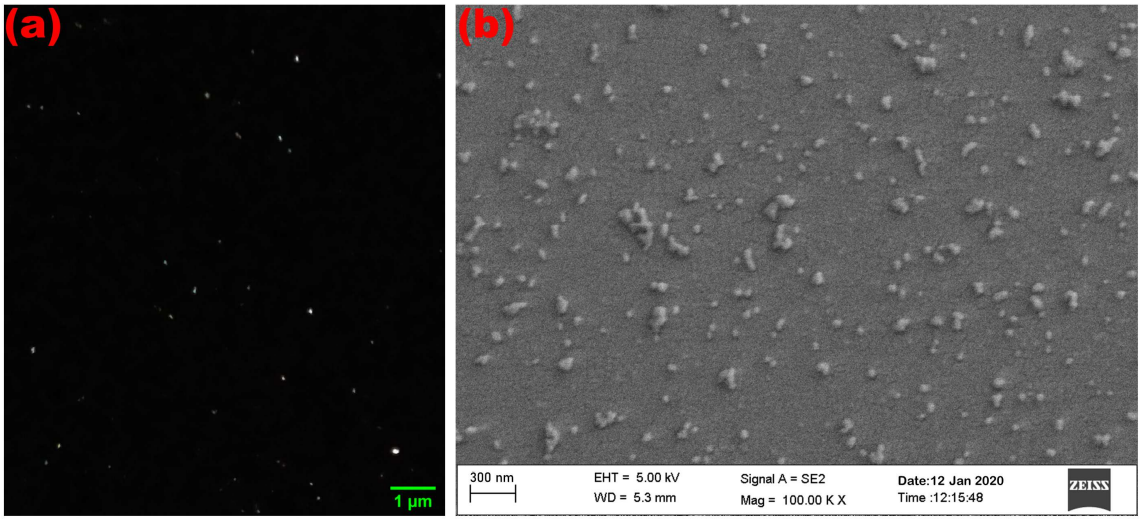

Figure 3.8: (a) TIRDF imaging of AuNPs using the designed smartphone microscopic system and (b) SEM image of the imaged AuNPs.

and the smartphone respectively.

In the next step of the present study, the DF mode of imaging of the proposed system has been evaluated. Figure 3.7 illustrates the DF images of the microbeads and HECCs as captured by the designed system under OIDF and TIRDF imaging modes. In OIDF imaging mode, the contrast and SNR values of the microbeads are estimated to be 0.96 and 42.06, respectively. On the other hand, with TIRDF imaging mode, the contrast and SNR values were found to be 0.98 and 90.5 respectively. The adjacent figures 3.7(b) and (d) represent the intensity profiles of the beads shown in the inset of figure 3.7(a) and (c) respectively. Clearly, amongst the different imaging modalities considered for the present study, a significant improvement in terms of contrast and SNR values for TIRDF imaging has been noticed. This is attributed to strong evanescent field scattering from the beads leaving behind a complete dark background. Figure 3.7(e) and (g) shows the images of HECC cells under OIDF and TIRDF illumination mode. The contrast and SNR values for OIDF are estimated to be 0.97 and 15.65, while in TIRDF mode these values are found to be 0.98 and 33.16 respectively. The intensity profiles of the marked cells are shown in figure 3.7(f) and (h) respectively. Here also, an enhanced performance of TIRDF mode over OIDF mode has been noticed. But, from the intensity plots shown in figure 3.7(f) and (h), a more detail information about the cell features can be seen under OIDF mode. The loss of information in TIRDF mode is attributed to the finite extension of the evanescent field (up to several hundred nanometers), which makes TIRDF technique suitable for surface inspection of transparent specimen.

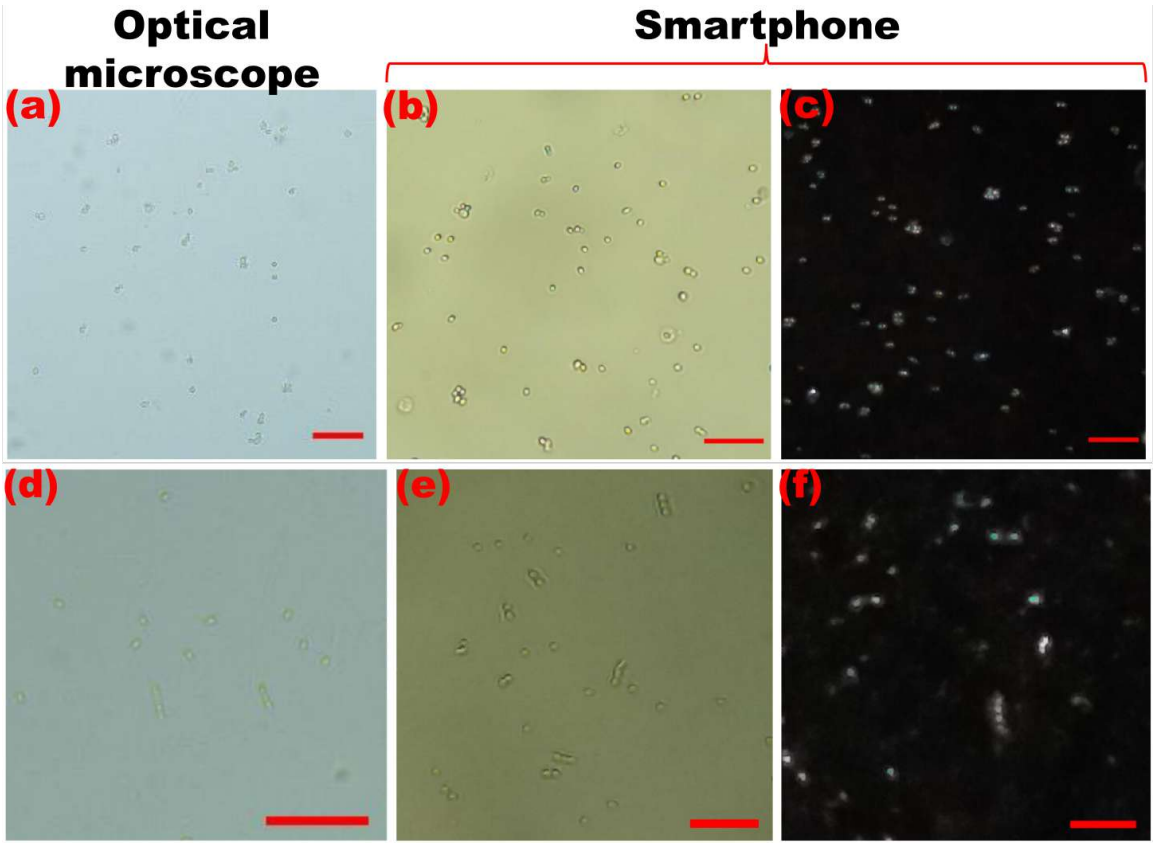

Figure 3.9: Applications of smartphone microscopic system for imaging of microorganisms. (a), (b) and (c) are the cropped and zoomed-in images of *C. albicans* acquired using a 10×/0.25NA objective lens, smartphone BF and OIDF imaging mode respectively. Scale bars are 50 μm. (d), (e) and (f) are the images of *B. subtilis* acquired using a 40×/0.45NA objective lens, smartphone BF and OIDF imaging mode, respectively. Scale bars are 20 μm.

3.5.2 Application of the microscopic tool to the imaging of nanoparticles

The applicability of the proposed smartphone platform microscopic system has been further evaluated for the imaging of nanoparticles in TIRDF mode. Gold nanoparticle (AuNP)s has been chemically synthesized in the laboratory using the standard chemical procedure [15]. Figure 3.8(a) represents the TIRDF imaging of the AuNPs recorded by the designed system. For imaging of the synthesized AuNPs, dilution has been performed and is taken on a highly cleaned standard microscopic slide. The SEM image of AuNPs as shown in figure 3.8(b) suggests that the dimension of the nanoparticle is varying in the range 60 nm to 250 nm. Due to poor scattering intensity, the OIDF imaging of AuNPs is not suitable with the proposed imaging setup. But in TIRDF imaging mode due to the interaction between evanescent field and the AuNPs, a strongly coupled localized surface plasmon resonance (LSPR) field is generated. Because of this unique resonance property of AuNPs, scattering efficiency enhances which can be recorded using our smartphone microscope.

3.5.3 Application to imaging of microorganisms

Imaging of living microorganisms is vital in microbiology applications. In the final step of the present study, label-free imaging of microorganisms has been carried out under BF and OIDF illumination conditions. Two species namely *C. albicans* and *B. subtilis* have been considered for imaging with the designed tool. *C. albicans* is a human fungal pathogen that causes *candidiasis* and has dimension between 10-12 μm in its yeast form. On the other hand, *B. subtilis* is a gram-positive bacterium found in gastrointestinal tract of ruminants and humans and has a physical dimension of approximately $\sim$0.25-1 μm in width. These two specimens thus become a good candidate to demonstrate the capability of the designed microscopic system. Cultured samples of both the species have been acquired from the Molecular Biology and Biotechnology (MBBT) department of Tezpur University and were diluted before imaging with the designed microscope.

In the present study, OIDF imaging mode has been chosen for dark-field imaging over TIRDF mode, because TIRDF imaging is suitable only when the samples are attached to the surface of the glass slide so that evanescent field, which extends few hundred nanometers, interacts effectively with the specimen. Figure 3.9(a), (b) and (c) show the images of *C. albicans* recorded by the standard microscope (10$\times$/0.25NA objective lens), and with BF and OIDF imaging mode of the designed smartphone tool, respectively. These captured images suggest that the smartphone platform microscope performs at par with that of traditional microscope. Again, figure 3.9(d), (e) and (f) show the comparison of the images of *B. subtilis* acquired by traditional

microscope (40×/0.45NA objective lens) and by the designed smartphone microscopic system. As can be seen from the figures, the proposed system can easily spatially resolve each of the considered bacteria species both in BF as well as in OIDF imaging mode. The motions of *C. albicans* under BF and OIDF imaging mode could also be visualized live under 'video mode' of the camera. It has been noticed that for the objects dimension below ∼1 μm, the proposed microscopic system while operating in BF and OIDF modes yield dimmer patterns in the final imaging due to defocusing. This is attributed to the limitation of the 3D-printing setup which has an optimal printing layer resolution of 10 μm and the roughness of the printing material. By incorporating a miniaturized translational dovetail stage for focusing, this issue can be avoided.

The imaging qualities of different microscopic particles captured by the designed tool suggest the versatility of the proposed platform which can be reliably used for imaging of all biological specimens. In this work, only the qualitative study of different specimens have been performed, which is a basic need for in-field study, whereas quantitative analysis such as cell counting of biological samples have been carried out in chapter 4 of the thesis work. DF illumination technique is widely used in the applications of plasmonic nanoparticles. However, particle size below the diffraction limit size cannot be detected with the conventional DF illumination technique. In such cases, TIRDF imaging is found to be an effective alternative platform for imaging of these particles [16, 17]. The sizes of the nanoparticles can also be determined by measuring the contrast of the scattering intensity using TIRDF technique [18].

3.6 Summary

In summary, a compact, multi-modal microscopic device using the integrated camera and LED flash modules of the smartphone has been demonstrated in this chapter using commercially available inexpensive lens system. One can switch rapidly from BF to OIDF and TIRDF imaging mode by changing the illumination optics in the setup. Due to the use of inexpensive elements such as iPhone 5s camera lens for magnification, plastic optical fibers for light guidance and 3D-printed setup; the overall cost involved for development of the device was USD 20 (excluding the smartphone) while maintaining its performance and functionality. It is envisioned that the designed microscopic system can be extended to other contrast-enhancing modalities such as polarized and fluorescence mode easily. The designed setup could emerge as a potential alternative platform for imaging of microorganisms and other submicron materials both in BF and DF modes.

References

[1] Gross, H. *Handbook of Optical Systems, Volume 1, Fundamentals of Technical Optics*, volume 1. 2005.

[2] Zuo, C., Sun, J., Feng, S., Hu, Y., and Chen, Q. Programmable colored illumination microscopy (pcim): a practical and flexible optical staining approach for microscopic contrast enhancement. *Optics and Lasers in Engineering*, 78:35–47, 2016.

[3] Murphy, D. B. *Fundamentals of light microscopy and electronic imaging*. John Wiley & Sons, 2002.

[4] Zuo, C., Sun, J., Feng, S., Zhang, M., and Chen, Q. Programmable aperture microscopy: A computational method for multi-modal phase contrast and light field imaging. *Optics and Lasers in Engineering*, 80:24–31, 2016.

[5] Ozcan, A. Mobile phones democratize and cultivate next-generation imaging, diagnostics and measurement tools. *Lab on a Chip*, 14(17):3187–3194, 2014.

[6] Lee, S. A. and Yang, C. A smartphone-based chip-scale microscope using ambient illumination. *Lab on a Chip*, 14(16):3056–3063, 2014.

[7] Tseng, D., Mudanyali, O., Oztoprak, C., Isikman, S. O., Sencan, I., Yaglidere, O., and Ozcan, A. Lensfree microscopy on a cellphone. *Lab on a Chip*, 10(14): 1787–1792, 2010.

[8] Pirnstill, C. W. and Coté, G. L. Malaria diagnosis using a mobile phone polarized microscope. *Scientific reports*, 5(1):1–13, 2015.

[9] Sung, Y., Campa, F., and Shih, W.-C. Open-source do-it-yourself multi-color fluorescence smartphone microscopy. *Biomedical optics express*, 8(11):5075–5086, 2017.

[10] Knowlton, S., Sencan, I., Aytar, Y., Khoory, J., Heeney, M., Ghiran, I., and Tasoglu, S. Sickle cell detection using a smartphone. *Scientific reports*, 5(1): 1–11, 2015.

[11] Switz, N. A., D'Ambrosio, M. V., and Fletcher, D. A. Low-cost mobile phone microscopy with a reversed mobile phone camera lens. *PloS one*, 9(5):e95330, 2014.

[12] Koydemir, H. C., Gorocs, Z., Tseng, D., Cortazar, B., Feng, S., Chan, R. Y. L., Burbano, J., McLeod, E., and Ozcan, A. Rapid imaging, detection and quantification of giardia lamblia cysts using mobile-phone based fluorescent microscopy and machine learning. *Lab on a Chip*, 15(5):1284–1293, 2015.

[13] Prieve, D. C. and Frej, N. A. Total internal reflection microscopy: a quantitative tool for the measurement of colloidal forces. *Langmuir*, 6(2):396–403, 1990.

[14] Braslavsky, I., Amit, R., Ali, B. J., Gileadi, O., Oppenheim, A., and Stavans, J. Objective-type dark-field illumination for scattering from microbeads. *Applied optics*, 40(31):5650–5657, 2001.

[15] Chamuah, N., Chetia, L., Zahan, N., Dutta, S., Ahmed, G. A., and Nath, P. A naturally occurring diatom frustule as a sers substrate for the detection and quantification of chemicals. *Journal of Physics D: Applied Physics*, 50(17): 175103, 2017.

[16] Cragg, G. E. and So, P. T. Lateral resolution enhancement with standing evanescent waves. *Optics letters*, 25(1):46–48, 2000.

[17] Qi, M., Darviot, C., Patskovsky, S., and Meunier, M. Cost-effective side-illumination darkfield nanoplasmonic marker microscopy. *Analyst*, 144(4):1303–1308, 2019.

[18] Yu, X., Araki, Y., Iwami, K., and Umeda, N. Measurement of nanoparticle sizes by conventional optical microscopy with standing evanescent field illumination. *Optics letters*, 33(23):2794–2796, 2008.